Packaging Effects on Fiber Bragg Grating Sensor Performance[1)]

HAO Jian-Zhong[1] TAKAHASHI Shiro[1] CAI Zhao-Hui[1] NG Jun Hong[1]
YANG Xiu-Feng[1] CHEN Zhi-Hao[1] LU Chao[2]

[1](*Institute for Infocomm Research,* 21 *Heng Mui Keng Terrace, Singapore* 119613*, Singapore*)
[2](*Nanyang Technological University, Nanyang Avenue, Singapore* 639798*, Singapore*)
(E-mail: {haoemily, vists, caizh, ngjh, yangxf, zchen}@i2r.a-star.edu.sg)

Abstract In this paper, the effects of packaging material and structure of fiber Bragg grating sensor performance are investigated. The effects of thermal expansion coefficient of different embedding materials on the temperature sensitivities of the FBG sensors are studied both theoretically and experimentally with good agreement, which provides a means for selection of FBG packaging material to achieve desired temperature sensitivity. We also demonstrate a 4-point bending structured FBG lateral force sensor that measures up to 242N force with well-preserved reflection spectrum, whereas for 3-point bending structure, multiple-peaks start to occur when applied force reaches 72N.

Key words Fiber bragg grating sensor, thermal expansion coefficient, lateral force sensor

1 Introduction

Fiber Bragg grating (FBG) sensors have been investigated intensively in the past few years due to its small size and robustness, ease of fabrication, suitability for use in multiplexed sensor networks and smart structures[1]. Based on the detection of wavelength change caused by the change of the effective refractive index and Bragg grating period, FBG can be used as sensors to measure temperature, strain, and displacement *etc.* Practical usage of FBG sensors is often limited by FBG′s sensitivity to both temperature and strain, which complicates independent measurement of each quantity. Therefore, discrimination of the effects between temperature and strain is essential in order to make accurate and reliable sensors.

Many techniques to discriminate the effects between strain and temperature have been reported. These include using superimposed gratings[2], a chirped Bragg grating[3], a long period grating[4], and FBG written in Hi-Bi optical fiber[5] *etc.* Among them a dual head sensor is one of the most effective schemes due to its compact size and good performance[6,7]. Although techniques using FBG[8] or fiber Fabry-Perot wavelength filter[9] as a demodulator have shown good results, they need a complete temperature-isolation of the demodulating FBG or a sophisticated calibration in fabricating the filter, respectively.

FBGs are usually embedded into modules on a variety of host materials for sensor′s protection as well as sensitivity enhancement. The performance of FBG sensors can be affected by the dominant parameters of the embedding materials such as thermal expansion coefficient (TEC), which can have direct influence on the temperature sensitivity of FBG sensors. Hence selection of embedding material becomes crucial for FBG sensors for achieving desired temperature sensitivity. However, very little study has been reported in the area. In section II of this paper, the effects of embedding materials on temperature sensitivity of FBG sensors are discussed both theoretically and experimentally with good agreements. The experimental results show that the FBG sensors packaged by large TEC material, such as Polymethyl Methacrylate (PMMA), can achieve 9 times more temperature sensitivity than that packaged by low/negative TEC material (such as CFRC — carbon fiber reinforce composite).

When used for force sensing as a stress element, FBG often exhibits low sensitivity to the force applied in the longitudinal direction of the fiber grating. One solution is to apply the force laterally to the FBG sensor module, where FBG can be surface-mounted or embedded into some host materials, and the FBG is located away from the neutral layer of the sensor module. Such structure provides a mechanism to enhance the FBG sensitivity to the applied force based on the bending concept. However, for the bending resulted from a single point-contact force, the reflection spectrum of the sensor will split into multiple peaks that decrease the accuracy and the dynamic range of the sensor. To solve the peak splitting problem in the FBG lateral force sensor to enable sensor interrogation with good accuracy and dynamic range, in Section 3 of this paper, we propose the use of 4-point bending concept

1) Supported by Science & Engineering Research Council of Singapore (052 118 0052)
Received February 8, 2006; in revised form March 10, 2006

for sensor construction. Investigation has been carried out to compare its performance with normal 3-point bending test method. The results show that FBG lateral force sensor under 4-point bending structure not only removes multiple peaks problem inevitable in 3-point bending structure but also increases the accuracy and the dynamic range of the lateral force sensor.

2 Fabrication of FBG

Fig. 1 shows the setup of FBG fabrication in our lab. It can write gratings with any profiles over a length of 40cm on many different types of fiber including normal single mode fiber, polarization maintaining fiber, multimode fiber and photonic crystal fiber. It is based on the principle of writing a subgrating per irradiation step. The UV-footprint creating this subgrating is accomplished by a phase mask. The fiber is translated with constant speed relative to the UV-fringes with an interferometer controlled translation stage. The position is very accurately tracked during the motion and this data is used to trigger the UV laser when the fiber reaches the desired position for the next irradiation.

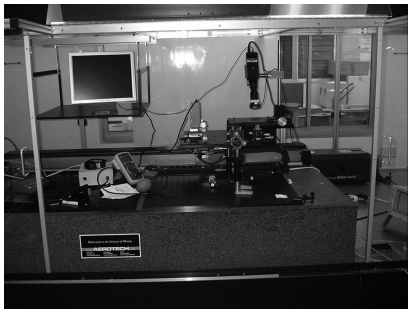

Fig. 1 FBG fabrication set-up using frequency-doubled argon laser and phase mask technique

A standard telecommunication grade single-mode optical fiber with a 250-micron acrylate coating (ITU-T G.652) is used for FBG fabrication. The fiber is hydrogen loaded to increase the photosensitivity. The acrylate coating of a short section (about 10∼20 mm) of the fiber are mechanically stripped off at pre-located position and the FBG is written into the stripped sections using a standard phase mask exposure technique. Blackmann-Harris apodisation is applied during grating writing to further improve the Gaussian profile of the reflection spectrum and suppress the formation of side-lobes. Each grating is 5-10 mm long and is located at the center of the stripped area. The number of FBGs along a single optical fiber can go up to several tens, provided the initial wavelength allocation of each sensor does not overlap with that of the adjacent sensors. The number of sensors depends on the sensitivity and the sensing range required by a particular application. It is also determined by the bandwidth and the power budget of the interrogation system. Immediately after FBG fabrication, all the FBGs are put into oven for annealing (100°C for 24 hours) to stabilize the Bragg wavelength. After annealing, necessary packaging are needed to form sensor modules. To make the entire sensor modules to be sensitive to the perpendicularly applied pressure/load/displacement, selection of packaging material and design of packaging structure play very important role. In this project, some fiber reinforced composite material is chosen for FBG sensor packaging due to their high strength-to-weight ratio, excellent corrosion resistance, high elasticity and excellent linear force translation, low electro-magnetic interference and easy to be molded into complex shapes.

3 Effects of thermal expansion coefficient of embedding materials on temperature sensitivities of FBG sensors

3.1 Theoretical discussion

Fiber Bragg grating is a periodic refractive index change along the core of the optical fiber; the periodic structure couples light from one fiber mode to another. An FBG reflects light that has a Bragg wavelength (λ_b) corresponding to twice its period (Λ), multiplied by the effective refractive index of the fiber (n) that the propagating mode sees.

$$\lambda_b = 2\Lambda n \tag{1}$$

This is called the Bragg condition. A change in the grating period will result in a change in the reflected wavelength. For this reason, FBGs are susceptible to any externally applied thermal-

mechanical loads that affect the grating period. Strain shifts the Bragg wavelength through expansion or contraction of the grating periodicity and through the strain-optic effect. Temperature change affects the Bragg response through thermal expansion and contraction of the grating periodicity and through the thermo-optic effect. These effects are well understood and, when adequately modeled, provide a means for predicting these changes. In other words, the sensing mechanism is the change in n and Λ caused by the measurands that are applied directly or indirectly to the FBG sensors or the sensor modules, and finally reflected by a change in λ_b. In this paper, the temperature and stress sensitivities are calculated based on (1).

Based on (1), the temperature and stress sensitivities are calculated for the embedded FBG sensor module. In the case where the module's TEC is different from the fiber's TEC, FBG will suffer internal stress (σ_i) induced by the temperature change. Considering the effect on λ_b shift, when externally applied stress is constant ($\sigma_e = \text{const}$), the temperature sensitivity can be obtained as

$$\frac{d\lambda_b}{dT} = 2\Lambda\left(\frac{\partial n}{\partial T_f}\cdot\frac{dT_f}{dT} + \frac{\partial n}{\partial \sigma_i}\cdot\frac{d\sigma_i}{dT}\right) + \frac{\lambda_b}{\Lambda}\left(\frac{\partial \Lambda}{\partial T_f}\cdot\frac{dT_f}{dT} + \frac{\partial \Lambda}{\partial \sigma_i}\cdot\frac{d\sigma_i}{dT}\right) \tag{2}$$

where T_f is the temperature of the fiber, which is equivalent to the module temperature T resulting $dT_f/dT = 1$, $\partial n/\partial T_f$ is the thermo-optic constant, $\partial n/\partial \sigma_i$ is the photo-elastic constant; $\partial\Lambda/(\Lambda\partial T_f) = \alpha_f$ is the TEC of the fiber; $\partial\Lambda/(\Lambda\partial\sigma_i) = 1/E_f$ where E_f is the fiber's Young's Modulus. Thus, the internal stress induced by the temperature change can be rewritten as

$$\frac{d\sigma_i}{dT} = \frac{d\sigma_i}{d\varepsilon_i}\cdot\frac{1}{l}\cdot\frac{dl_m - dl_f}{dT} = E_f(\alpha_m - \alpha_f) \tag{3}$$

where dl_m and dl_f are the length change of the module and the fiber at free stress condition, respectively; ε_i is the internal strain from the original free length at a temperature and lastly α_m is the TEC of the module. Therefore, (2) is summarized as

$$\frac{d\lambda_b}{dT} = 2\Lambda\left\{\frac{\partial n}{\partial T_f} + \frac{\partial n}{\partial \sigma_i}\cdot E_f\cdot(\alpha_m - \alpha_f)\right\} + \lambda_b\alpha_m \tag{4}$$

From (4), it can be concluded that larger α_m gives higher temperature sensitivity and smaller or negative α_m gives lower temperature sensitivity of the module. If $\alpha_m = \alpha_f$ then (4) becomes (5) as follows.

$$\frac{d\lambda_b}{dT} = 2\Lambda\frac{\partial n}{\partial T_f} + \lambda_b\alpha_f \tag{5}$$

(5) is the same as the equation reported by Kenji Kintaka[10] where photo-elastic effect is neglected. When the temperature surrounding the FBG sensor module is constant, the stress sensitivity becomes

$$\frac{d\lambda_b}{d\sigma_e} = 2\Lambda\frac{dn}{d\sigma_e} + \frac{\lambda_b}{\Lambda}\frac{d\Lambda}{d\sigma_e} = 2\Lambda\frac{dn}{d\sigma_e} + \lambda_b\frac{1}{E_f} \tag{6}$$

where σ_e is the stress caused by the external force, so $dn/d\sigma_e$ shows the same value as the fiber's photoelastic constant and $d\Lambda/(\Lambda d\sigma_e) = 1/E_f$. Using the relation of $d\sigma_e = E_f d\varepsilon$, where ε is the strain of FBG, we can obtain the strain sensitivity as follows.

$$\frac{d\lambda_b}{d\varepsilon} = 2\Lambda\cdot\frac{dn}{d\sigma_e}\cdot E_f + \lambda_b \tag{7}$$

Above equation shows that the strain sensitivity is a constant when the grating structure and the material of FBG fiber are identified.

3.2 Experimental verifications

In order to confirm the fiber parameters such as thermo-optic constant and photo-elastic constant, some bare FBGs written on hydrogen-loaded single-mode fiber (SMF) were investigated. The temperature sensitivity ($d\lambda_b/dT$) and strain sensitivity ($d\lambda_b/d\varepsilon$) were measured to be 10.9 pm/°C and 1.1 pm/$\mu\varepsilon$, respectively. The strain sensitivity obtained here is in good agreement with the reported value of 1.15 pm/$\mu\varepsilon$[11] whereas the temperature sensitivity of 10.9 pm/°C is different from the reported value of 13 pm/°C. Base on our result, by substituting the parameters of $\lambda_b = 1550$nm, $\Lambda = 533$nm, $E_f = 70$GPa and $\alpha_f = 7\times10^{-7}$/°C into (5) and (7), we can calculate

$$dn/dT = 0.9\times10^{-5}/^{\circ}C,\ where\ \sigma = const, \quad dn/d\sigma = -6\times10^{-3}/GPa,\ where\ T = const$$

The negative value of photo-elastic constant means the refractive index decreases with increased tensile stress. Based on the composition dependence of thermo-optic constant, it is understood from previous calculation that Morey′s value corresponded to germanium-doped silica ($dn/dT = 1.1 \times 10^{-5}/^{\circ}\mathrm{C}$) and our experimental result corresponded to germanium-boron co-doped silica ($dn/dT = 0.9 \times 10^{-5}/^{\circ}\mathrm{C}$).

Next, experiments to find the effects of module materials on the temperature sensitivity were carried out. Firstly, polymethyl methacrylate (PMMA), a sort of acrylate polymer was chosen to be the module material for FBG sensors due to its large α_m. Structures of the samples are shown in Fig. 2. In both structures, an FBG was embedded into a small groove on a PMMA plate and fixed with hard epoxy resin; the only difference is that the FBG was then covered by another PMMA plate to form a sandwitch structure for sample A1. For sample A2, the FBG was just surface mounted with epoxy. The results are shown in Fig. 3. Temperature sensitivity for A1 and A2 were measured to be 101pm/°C and 91pm/°C, respectively, which are about nine times larger than that of a bare FBG, due to a larger α_m value for the PMMA. Using this result and (4), the TEC of the PMMA is calculated to be $0.8 \times 10^{-4}/^{\circ}\mathrm{C}$, which is in good agreement with the typical value of around $1 \times 10^{-4}/^{\circ}\mathrm{C}$.

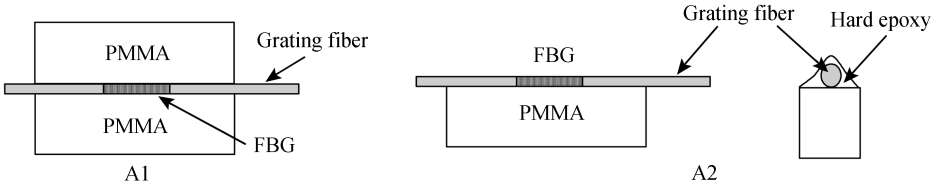

(A1) Sandwiched in between two PMMA plates (A2) Attached to the surface of a PMMA plate with some hard epoxy

Fig. 2 FBG is fixed with hard epoxy resin

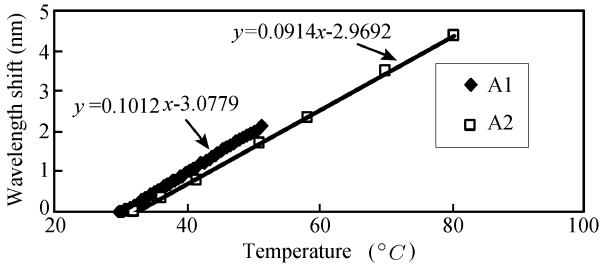

Fig. 3 Comparison of temperature sensitivity between FBG sensor modules A1 and A2

Secondly, the effects of carbon fiber reinforced composite (CFRC) material on the module temperature sensitivity were studied. Two sensor modules consisting layers of unidirectional CFRC (Fiberdux 913C-XAS) with FBG embedded at 0° (sample C_0) and 90° (sample C_{90}) to the carbon fibers as shown in Fig. 4.

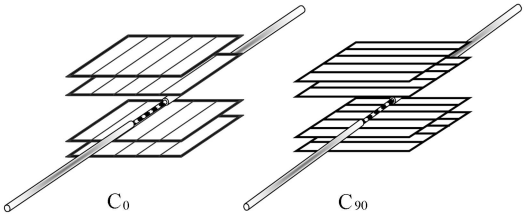

Fig. 4 FBG embedded into CFRC, with grating fiber running 0° (C_0) and 90° (C_{90}) to the carbon fiber

From Fig. 5, the temperature sensitivities for C_0 and C_{90} were measured to be 9.9 pm/°C and 53 pm/°C respectively. The difference in the two sensitivities is caused by the different TEC values in the 0° and 90° directions. The composite laminate at 0° direction has a TEC of $-1 \times 10^{-7}/^{\circ}\mathrm{C}$. Substituting

this value into (4), the temperature sensitivity for sample C_0 is calculated to be 9.8pm/°C, which is very close to the value obtained experimentally. Conversely, by using experimentally obtained temperature sensitivity of 53pm/°C, the TEC is calculated to be 39×10^{-6}/°C in 90° direction of CFRC, where the effect of matrix becomes dominant. This result seems quite reasonable as compared to the typical TEC value of around 32×10^{-6}/°C of the CFRC in which the carbon and matrix volume ratio is 6:4.

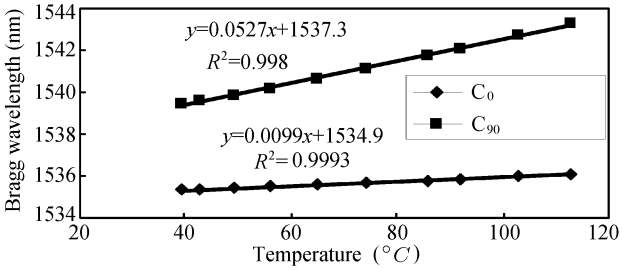

Fig. 5 Comparison of temperature sensitivity between CFRC embedded FBG sensor modules C_0 and C_{90}

4 A robust FBG lateral force sensor based-on 4-point bending concept

4.1 Principle

The structures of 3-point and 4-point bending tests for sensor construction are shown in Fig. 6. In 3-point bending, a single point force is applied to part of the grating. While for 4-point bending, a two-point force outside the grating region is applied. The grating strains along the first halves of the beams ($x \leqslant 0.5$a) can be derived from the original equation[12] to become

$$\varepsilon_3(x) = \frac{Fxd}{2IE} \equiv k_1 x F \tag{8}$$

$$\varepsilon_4(x) = \frac{F(a-c)d}{4IE} \equiv k_2 F \tag{9}$$

$$I = \frac{wt^3}{12} \tag{10}$$

where w is the width of the FBG package, d is the distance from the neutral layer of the laminate to the fiber, E is the Young′s Modulus and I is the second moment of the beam′s cross section. Other parameters are indicated in Fig. 5. As the size of the fiber is small, its effect on the mechanical properties of host material is negligible.

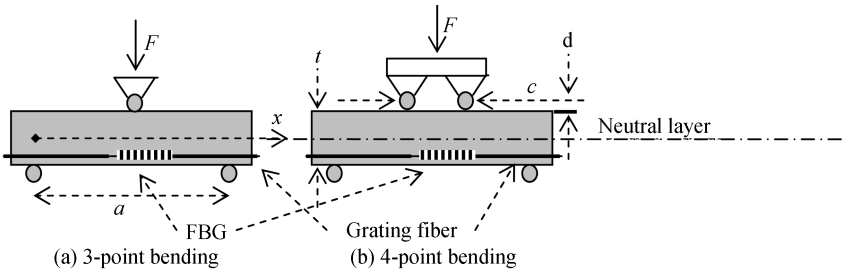

Fig. 6 Structure of 3-point bending and 4-point bending

In the case of 3-point bending, we find that the strain $\varepsilon_3(x)$ is proportional to x that causes the strain gradient $\partial\varepsilon/\partial x$ along the grating, at the same time; a broadening in the reflection bandwidth is expected due to the strain gradient along the grating by using the equation of Bragg reflection against strain[13]:

$$\lambda_B = \lambda_{Bo}(1 + k\varepsilon) \tag{11}$$

This equation means that the bandwidth and the side-lobe power of the reflection spectrum will increase due to the strain distribution along the grating. On the contrary, 4-point bending shows uniform strain along the grating, hence only the shift of the reflection spectrum is expected due to the uniform strain along the grating.

4.2 Experimental setup

When used for sensing applications, FBGs are usually embedded into a variety of host materials for protection as well as sensor performance enhancement[14]. One commonly used material is carbon fiber reinforced composite (CFRC) due to its mould ability, high strength-to-weight ratio and excellent corrosion resistance. It is also a good elastic embedding material for force detection sensor modules. To study the bending effects on the performance of FBG lateral force sensor, an FBG is embedded into 8 layers of uni-ply CFRC material with the grating fiber running parallel to the carbon fiber in a stacking sequence of 0/0/0/0/0/0/0/FBG/0. The experimental setup is shown in Fig. 7, an FBG Interrogation System (FBGIS) from Micron Optics Inc (Model Si425) and an Optical Spectrum Analyzer (OSA) from Advantest (Model Q8384) are used to measure the peak wavelength and reflection spectrum from the FBG sensor respectively. An LF-Plus Series Advanced Digital Testing System from Chatillon is used to conduct 3-point and 4-point bending tests. The parameters (w, t, a, d, c, k) reflected in Fig. 6 and (8)∼(11) are shown in Table 1.

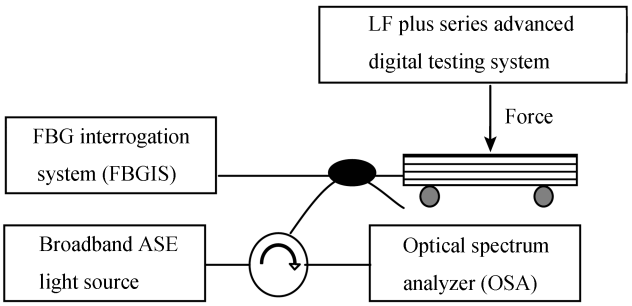

Fig. 7 Experimental setup for the FBG lateral force sensor module

Table 1 Parameters for 3-point and 4-point bending set-up

Embedding Structure for FBG lateral force sensor	w mm	t mm	a mm	d mm	c mm	k
0/0/0/0/0/0/0/FBG/0	12.0	1.64	50	0.68	15	0.78

4.3 Results

4.3.1 Results from FBGIS (FBG interrogation system)

Fig. 8 depicts the wavelength shifts obtained from the FBGIS when the FBG sensor is under 3-point and 4-point bending tests. The relationship between wavelength shift and applied force is found to be 99.9% when linear fitted. Although 3-point bending allows a high force dynamic range up to 200 N, a second peak starts to appear when the applied force rises above 72 N, which is undesirable because the second peak confuses the FBGIS. In the case of 4-point bending, a dynamic sensing range up to 242 N of the applied force (equivalent to 4nm of the peak wavelength shift) is obtained without any second peak occurrence.

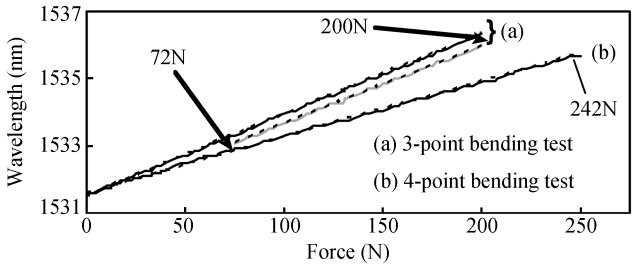

Fig. 8 FBG peak wavelengths versus applied forces under (a) 3-point bending; (b) 4-point bending

4.3.2 Results from OSA (Optical spectrum analyzer)

Fig. 9(a) shows the reflection spectrum when a lateral force is applied to the 3-point bending structure. When the FBG is under tension/compression, the Bragg wavelength experiences a red/blue

shift. This is due to the positive/negative strain along the grating. The negative force means that the sensor module is flipped over hence the fiber is under compression. When no force is applied, the side-lobes′ power spectral densities (PSDs) are smaller as compared to the main-lobe. However, when a force is applied, the reflection bandwidth increases. At the same time, the side-lobes′ PSDs increase in comparison to the main-lobe due to broadening of the reflection spectrum. When the force is lower than -265N, the PSDs of side-lobes become higher than that of the main lobe, which confuses the FBGIS and results in false peak detection. When the applied force is extremely large, the whole spectrum deteriorates as shown in Fig. 9(a).

Fig. 9(b) shows the result of an FBG sensor module under 4-point bending test. The single-peak of the reflection spectrum is well-maintained at large magnitudes of the applied force. The small distortion of the reflection spectrum (in the case of compression) could be due to high asymmetric arrangement of the sensors. 4-point structure offers a dynamic sensing range up to 4nm of wavelength shift or 242N of applied force, which is three times more than that obtained from 3-point bending test., Measurements were conducted only up to 300N due to equipment limitation. However, even at 300N, the spectrum is still well preserved. Furthermore, as 4-point structure always induces a uniform strain along grating, the structure can have a dynamics range up to fracture/failure point of the sensor module. This result shows that wider dynamic range can be achieved by using 4-point bending approach.

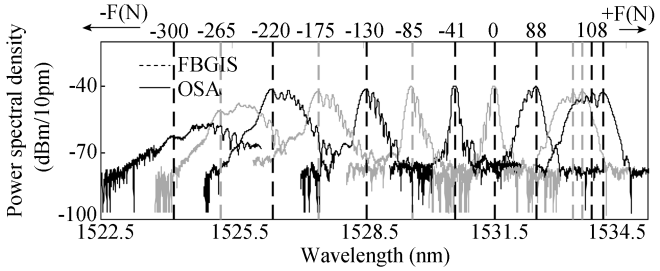

(a) 3-point bending test

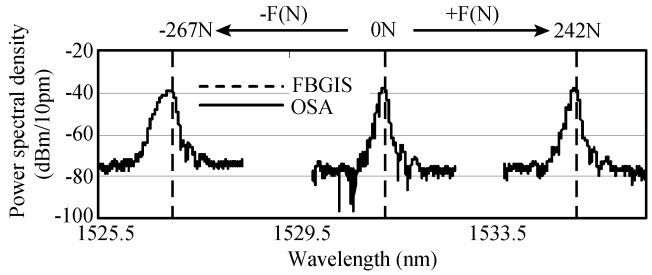

(b) 4-point bending test

Fig. 9 Reflection spectrum and Bragg wavelength of the FBG lateral force sensor under 3-point and 4-point bending tests

4.4 A robust 4-point bending structured FBG lateral force sensor

Based on the encouraging results obtained above, a robust FBG lateral force sensor has been constructed based on the 4-point bending concept as shown in Fig. 10. Firstly a 5 mm long FBG is embedded into a 50 mm long flat shape CFRC laminate; secondly 2 pillars are symmetrically secured to one side of the laminate using some hard epoxy. Finally a 10 mm long block is attached to the center of the other side of the laminate using some soft resin, to cover the FBG area. The sensor is calibrated and the results show that this sensor can measure lateral force up to 250 N with excellent linearity between the Peak wavelength of the FBG sensor and laterally applied force.

5 Conclusion

To clarify the temperature sensitivity of FBG sensor module theoretically, the effect of the internal stress induced by the temperature change was studied. The sensitivity to the stress applied to the fiber

was also theoretically derived and the strain sensitivity was found to be always constant when the FBG structure and material are identified. For the sensor modules embedded in PMMA, the experimental results have shown that the temperature sensitivities are about nine times larger than that of the bare FBG. In the case of FBG embedded in negative TEC material such as uni-directional CFRC in parallel direction (sample C0), it was confirmed experimentally that the temperature sensitivity of the module was smaller than that of the bare FBG.

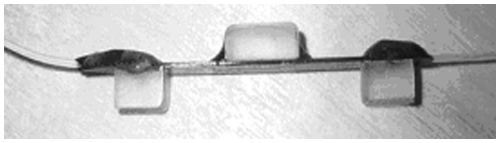

(a) Picture showing side-view

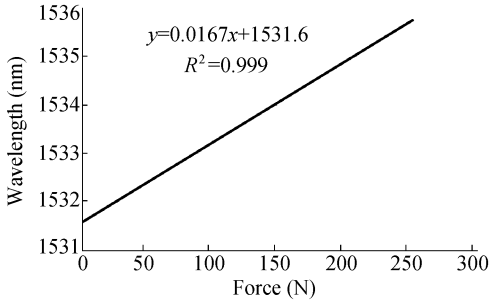

(b) Calibration results between Peak wavelength of FBG sensor and laterally applied force

Fig. 10 A 4-point bending structured FBG lateral force sensor

An FBG lateral force sensor has been investigated using 3-point and 4-point bending tests. The results show that the FBG lateral force sensor with 4-point bending structure not only removes multiple peaks problem faced by 3-point bending structure but also increases the accuracy and the dynamic range of the lateral force sensor. As a result, a robust FBG lateral force sensor has been constructed based on 4-point bending concept, which will be more feasible for applications where high dynamic range and sensitivity are required.

From the theoretical analysis and experimental evaluations of section II and III of this paper, we conclude that the packaging material often plays dominant role for FBG sensors because the sensor module performance such as temperature sensitivity or strain sensitivity can be directly affected by the material constants (such as thermo-optic constant, photo-elastic constant and TEC) of the host surrounded FBG. Besides the selection of packaging material, the structure of the sensor module is also very important as it can affect the accuracy and dynamic sensing range of the sensor module. Furthermore, how to mount the sensor module onto the object is also critical because the sensor performance can be affected by the mounting conditions too.

References

1 Kersey A D, Davis M A, Patrick H J, LeBlanc M, Koo K P, Askins C G, Putnam M A, Friebele E J. Fiber grating sensors. *Lightwave Technology*, 1997, **15**(8): 1442∼1463

2 Xu M G, Archambault J L, Reekie L, Dakin J P. Discrimination between strain and temperature effects using dual-wavelength fiber grating sensors. *Electronics Letters*, 1994, **30**(13): 1085∼1087

3 Xu M G, Dong L, Reekie L, Tucknott J A, Cruz J L. Temperature-independent strain sensor using a chirped Bragg grating in a tapered optical fiber. *Electronics Letters*, 1995, **31**(10): 823∼825

4 Bhatia V, Campbell D, Claus R O, Vengsarkar A M. Simultaneous strain and temperature measurement with long-period gratings. *Optics Letters*, 1997, **22**(9): 648∼650

5 Chen G H, Liu L Y, Jia H Z, Yu J M, Xu L, Wang W C. Simultaneous strain and temperature measurements with Bragg grating written in novel Hi-Bi optical fiber. *IEEE Photonics Technology Letters*, 2004, **16**(1): 221∼223

6 James S W, Dockney M L, Tatam R P. Simultaneous independent temperature and strain measurement using in-fiber Bragg grating sensors. *Electronics Letters*, 1996, **32**(12): 1133∼1134

7 Song M, Lee S B, Choi S S, Lee B. Simultaneous measurement of temperature and strain using two fiber Bragg gratings embedded in a glass tube. *Optical Fiber Technological*, 1997, **3**(2): 194∼196
8 Jackson D A, Lobo Ribeiro A B, Reekie L, Archambault J L. Simple multiplexing scheme for a fiber-optic grating sensor network. *Optics Letters*, 1993, **18**(7): 1192∼1194
9 Kersey A D, Berkoff T A, Morey W W. Multiplexed fiber Bragg grating strain-sensor system with a fiber Fabry-Perot wavelength filter. *Optics Letters*, 1993, **18**(16): 1370∼1372
10 Kintaka K, Nishii J, Kawamoto Y, Sakamoto A, Kazansky P G. Temperature sensitivity of Ge-B-SiO_2 waveguide Bragg gratings on a crystallized glass substrate. Optics Letters, 2002, **27**(16):
11 Morey W W, Dunphy J R, Meltz G. Multiplexing fiber Bragg gratings sensors. In: Proceedings of SPIE. Boston: SPIE, 1991. **1586**: 216∼224
12 Ferdinand P. Beer, *et al.*, Mechanics of Materials, Mc Graw Hill, 3rd edition, 2002, 217
13 Falciai R, Trono C. Curved elastic beam with opposed fiber-bragg gratings for measurement of large displacements with temperature compensation. *IEEE Sensors Journal*, 2005, **5**(6): 1310∼1314
14 Kuang K S C, Whelan M P, Kenny R, Cantwell W J, Chalker P R. Embedded fiber Bragg gratings in advanced fiber composite materials. *Composite Science and Technology*, 2001, **61**: 1379∼1387

HAO Jian-Zhong Received her Ph. D. degree from Nanyang Technological University, Singapore. Currently she is a senior research fellow at Institute for Infocomm Research in Singapore. Her research interests include fiber optic sensors and components, system integration, and MEMS and fiber radio.

TAKAHASHI Shiro Received his Ph. D. degree from Waseda University in Japan, in 1980. He is a senior research fellow at Institute for Infocomm Research in Singapore. His research interests include fiber optic sensors and optical components.

CAI Zhao-Hui Received his Ph. D. degree from Beijing University of Posts and Telecommunications in 1998. Now he is a research scientist at Institute for Infocomm Research, Singapore. His research interests include optical communications, channel coding, and modulation.

NG Jun Hong Received his master degree from Nanyang Technological University in 2000. He is a senior research engineer at Institute of Infocomm Research, A*STAR. His research interests include sensor application and fabrication technique of fiber bragg grating.

YANG Xiu-Feng Received her Ph. D. degree from Nankai University in 1998. She is a research scientist in Institute for Infocomm Research, Singapore now. Her research interests include optical fiber laser, fiber bragg grating device, and optical fiber sensing system.

CHEN Zhi-Hao Received his bachelor, master, and Ph. D. degrees from East China Normal University, Shanghai University of Science and Technology, and Tsinghua University, respectively. His research interests include fiber and integrated optics, optical sensors and their applications.

LU Chao Received his bachelor degree from Tsinghua University in 1985 and his Ph. D. degree from University of Manchester in 1990. He is an associate professor at Nanyang Technological Univesrity, Singapore. He was with Institute for Infocomm Research, Singapore from 2002-2005. His research interests include fiber devices and optical communication systems.